Advances in Nano Research, *Vol. 10, No. 5 (2021) 481-491*
DOI: https://doi.org/10.12989/anr.2021.10.5.481

Nonlinear vibration of nanosheets subjected to electromagnetic fields and electrical current

Tayyeb Pourreza[1a], Ali Alijani[*1], Vahid A. Maleki[1,2b] and Admin Kazemi[1c]

[1]*Department of Mechanical Engineering, Bandar Anzali Branch, Islamic Azad University, Bandar Anzali, Iran*
[2]*Department of Mechanical Engineering, University of Tabriz, Tabriz, Iran*

(*Received December 19, 2020, Revised January 26, 2021, Accepted January 28, 2021*)

Abstract. Graphene Nanosheets play an important role in nanosensors due to their proper surface to volume ratio. Therefore, the main purpose of this paper is to consider the nonlinear vibration behavior of graphene nanosheets (GSs) under the influence of electromagnetic fields and electrical current create forces. Considering more realistic assumptions, new equations have been proposed to study the nonlinear vibration behavior of the GSs carrying electrical current and placed in magnetic field. For this purpose, considering the influences of the magnetic tractions created by electrical and eddy currents, new relationships for electromagnetic interaction forces with these nanosheets have been proposed. Nonlinear coupled equations are discretized by Galerkin method, and then solved via Runge–Kutta method. The effect of different parameters such as size effect, electrical current magnitude and magnetic field intensity on the vibration characteristics of GSs is investigated. The results show that the magnetic field increases the linear natural frequency, and decreases the nonlinear natural frequency of the GSs. Excessive increase of the magnetic field causes instability in the GSs.

Keywords: graphene nanosheets; vibration analysis; nonlinear frequency; magnetic traction; electric and eddy currents

1. Introduction

With the development of nanotechnology (Khodashenas 2015, Rezaee and Maleki 2015, Salimi *et al*. 2015, Kheradmandan and Barati 2017, Aydogdu *et al*. 2018), GSs play a very important role in actuators and sensors due to their very special properties. Graphene has become a unique material due to its extraordinary properties such as: thermal, optical conductivity and electrical, high density and excellent mechanical properties (Rezaei *et al*. 2020). Due to the fact that these materials can have ferromagnetic properties, the use of these plates in a wide range of applications of photonic, electronic and mechanical nanosensors as the most important nanoelectromechanical systems (NEMS), has been considered (Sia 2013, Cicek and Nadaroglu 2015, Ebrahimi *et al*. 2018, Mohammadian *et al*. 2019, Le 2020, Attar *et al*. 2021). One of the newly developed nanostructure is nano-plate, which has various applications in sensors (Tezerjani *et al*. 2017, Bendaho *et al*. 2019, Karami and Karami 2019) and actuators (Ponmozhi *et al*. 2012, Fakhrabadi *et al*. 2015, Lu *et al*. 2019). For example, self-powered mass sensor based on electro-magnetic nanoplate was investigated for identification of small masses by Asadi *et al*. (2017). Umar *et al*. (2021) conducted the fabrication and characterization of CuO nanosheets based sensor device for ethanol gas sensing application. Chen *et al*. (2019) presented an electro-thermo-mechanical coupling system of micro/nano-scale bistable plates for piezoelectric energy-harvesting applications.

A review of the studies on vibrational behavior of ferromagnetic sheets shows that the major studies in this field are related to metric plates, and very limited studies have investigated the conductive nanosheets. Murmu and Pradhan (2009) applied the nonlocal elasticity theory to investigated the vibration behavior of GSs. Mohammadi *et al*. (2014) studied the free vibrations of graphene sheets under radial compressive load and temperature changes. In their study, graphene sheets were placed on the elastic substrate, and the nonlocal elasticity theory was used to model the problem. Kumar *et al*. (2013) investigated the thermal induced vibrations of a monolayer graphene sheet on a polymeric elastic substrate using nonlocal shell theory. The nonlinear vibrational behavior for a rectangular simply supported monolayer graphene sheet in thermal environment is proposed by Shen *et al*. (2010). Fazelzadeh *et al*. (2014) analyzed the thermomechanical vibrations of orthotropic nanosheets. Farajpour *et al*. (2011) studied the buckling of graphene nanosheets on Winkler-Pasternac elastic foundation using the nonlocal elasticity theory. Using the Levy solution model, Samaei *et al*. (2011) extracted the bending response of graphene monolayer sheets under temperature and external mechanical loads. Pradhan (2009) discussed the buckling behavior of rectangular monolayer GSs using the nonlocal elastic rectangular sheet model and the theory of high-order shear

∗Corresponding author, Ph.D.,
E-mail: alijani@iaubanz.ac.ir,
Postal Code: 43131, Fax: +98 134 440 0486.
[a]Ph.D. Student, E-mail: t_pourreza@iaul.ac.ir
[b]Ph.D., E-mail: vahid_maleki@tabrizu.ac.ir
[c]Ph.D., E-mail: admin.kazemi@gmail.com

ISSN: 2287-237X (Print), 2287-2388 (Online)

deformation considering quantum effects. The nonlocal first-order shear deformation elasticity theory is used for buckling of a single-layered graphene sheet embedded in visco-Pasternak by Zenkour (2016). Bouadi *et al*. (2018) a nonlocal higher order shear deformation theory (HSDT) developed for buckling properties of single graphene sheet. Chandra *et al*. (2020) suggested a sandwich beam model to investigate the vibrations of bilayer GSs by considering the interlayer shear effect. Tao *et al*. (2020) based on the higher-order shear deformation theory investigated the nonlinear vibrations of functionally graded graphene platelets-reinforced composite in the thermal loads. Ansari and Ajori (2015) and Ansari *et al*. (2015, 2016) considered the effects of surface stress on post-buckling modeling, vibration behavior, and instability of a circular nanosheet. Using Kirchhoff's thin sheet theory, Assadi (2013) analytically investigated the forced vibrations of a rectangular nanosheet by considering the surface effects. Shafiei *et al*. (2020) studied the small size effect on vibration response and mechanical buckling of single layered GSs based on two variable plate theory. Using the theory of nonlocal elasticity, Naderi *et al*. (2014) studied the vibration analysis and elastic stability of biaxially loaded GSs. Using the nonlocal elasticity theory, Barretta *et al*. (2019) considered the small size effect on stress distributions of homogeneous thin nanosheets. They derived the motion equations using classical sheet theory, assuming von Kármán's nonlinear displacement-strain relations. Ghadiri *et al*. (2018) analytically studied the steady-state dynamics of a rectangular GSs resting on a viscoelastic substance under thermo-mechanical- magnetic forces via the Kirchhoff plate model and nonlocal Eringen's theory. Ajri *et al*. (2018) analytically analyzed the non-stationary free vibration and nonlinear dynamic behavior of the viscoelastic nano-sheets. Singh and Azam (2020) investigated vibration behavior of a nanosheet using Eringen's nonlocal plate theory. The governing equations of nanosheet have been derived using the principle of virtual work, and the solution is obtained using the Rayleigh–Ritz method and characteristic polynomials. A multiple-scale perturbation method is employed to analyze nonlinear free vibration of nanoplate incorporating surface effects by Allahyari *et al*. (2020). Ajri and Seyyed Fakhrabadi (2018) studied the nonlinear free vibration of viscoelastic nanoplates based on modified couple stress theory. In most conditions of severe environments, when the nanosheet deflection-to-thickness ratio is greater than 0.4, the nonlinearity is very important and should be given consideration. Therefore, the nonlinear free and forced vibration of nanosheet subjected to different loads has given rise to a number of studies (Shen and Huang 2007, Al-Furjan *et al*. 2021, Salmani *et al*. 2021).

Most existing studies in the literature examine the dynamic behavior of nanosheets under different types of forces by various numerical and analytical methods (Saremi *et al*. 2013, Vahidi Pashaki *et al*. 2018, Ghannadpour and Moradi 2019, Wong *et al*. 2019, Kachapi 2020, Mehrez *et al*. 2020). Many works presented in the literature include the vibration behavior of a nanosheets under electrical currents, as well as eddy currents generated by magnetic field. Furthermore, the dynamic behavior of ferromagnetic GSs located under the magnetic fields, has not been studied. Accordingly, in the present study, considering the interaction between ferromagnetic material, magnetic field and magnetic traction generated by electric currents, a new magneto-electro-mechanical coupled equations are provided to study the flexural vibration of ferromagnetic GSs carrying electric current and located in magnetic field. For this purpose, the equations of motion are derived using von Kármán's nonlinear displacement-strain relations. The solutions obtained by the Galerkin and Runge–Kutta method are presented herein. Using these equations, the nonlinear vibration response of GSs is studied.

2. Equations of motion

According to Fig. 1, a rectangular ferromagnetic GSs with length a, thickness h and width b is investigated to carry electrical current along the axial axis (x-axis). Amount of the vertical magnetic field and the external force are B_0 and $q(t)$, respectively.

2.1 Equations of magnetic fields

Basic equations including Biot–Savart law, Ampere law and Cauchy's relations are used for linear and angular momentum equilibrium equations to solve the dynamic problems of magnetoelastic systems (Trimarco and Maugin 2001, Chung 2007)

$$\begin{aligned} &t^E_{ij,i} + \rho\left(f_j - \dot{v}_j\right) + F^E_j = 0, \\ &e_{ijk}t^E_{ij} = c^{em}_k, B_{i,i} = 0, e_{ijk}H_{j,k} = 0 \end{aligned} \tag{1}$$

where t^E_{ij}, F^E_j, f_j, v_j and c^{em}_k are the elastomagnetic stress tensor, electromagnetic body force, the mechanical body force, velocity vector and electromagnetic momentum, respectively. e_{ijk}, B_i and H_i are the permutation tensor, indicate density of magnetic flux and intensity of the magnetic field, respectively. In the present study, $B_i = \mu_0(H_i + M_i)$, in which $\mu_0 = 4\pi \times 10^{-7}\frac{N}{A^2}$ and M_i are vacuum permeability between the two materials and the magnetization vector, respectively.

Maxwell equations are used to calculate the electromagnetic stresses and the electromagnetic force inside the sheet. According to Maxwell's classical relations (Arani *et al.* 2013)

$$\begin{aligned} &\left[-M_iB_j + t^E_{ij}\right]n_j = 0, \nabla \cdot \boldsymbol{B} = 0 \\ &\nabla \times \boldsymbol{H} = \boldsymbol{J}_f, \boldsymbol{n} \times [\boldsymbol{H}] = 0, \boldsymbol{M} = \chi_m \boldsymbol{H}, \boldsymbol{H} = \frac{1}{\mu_0}\boldsymbol{B} \end{aligned} \tag{2}$$

in which $t^E_{ij}, \boldsymbol{n}$, $\boldsymbol{J}_f, \boldsymbol{H}$, $\boldsymbol{M}$ and χ_m are elastomagnetic stress tensor, unit vector normal to the surface, current density, magnetic field distribution vector, magnetization constant and susceptibility of the ferromagnetic medium ($\chi_m(= 10^2 - 10^5) >> 1$ for linear soft ferromagnetic materials), respectively (Maugin 2013).

Assuming the material to be conductive, polarization for the sheet is zero, and on the other hand, assuming that there

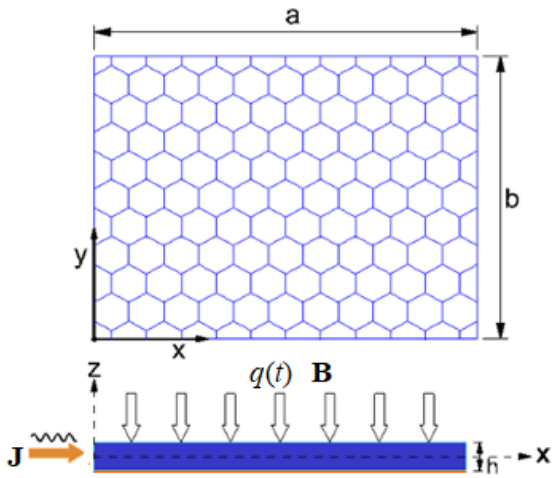

Fig. 1 Ferromagnetic GSs subjected to the magnetic field and electrical current

is no point charge in the problem, the macroscopic electromagnetic body force, $\boldsymbol{F}^{EM}$, created by the electrical current passing through the GSs subjected to the magnetic field is achieved as

$$\boldsymbol{F}^{EM} = \nabla \boldsymbol{B} \cdot \boldsymbol{M} + \boldsymbol{J} \times \boldsymbol{B} \tag{3}$$

Since in this study the electromagnetic momentum is not a function of time, the relationship among momentum, electromagnetic stress components and force is given by

$$\boldsymbol{F}^{EM} = \nabla \cdot \boldsymbol{t}^{EM} \tag{4}$$

Considering the Maxwell and electromagnetic stress tensor as ${t_{ij}}^{Maxwell}$ and ${t_{ij}}^{EM}$, the electromagnetic stress tensor is achieved as

$${t_{ij}}^{E} = {t_{ij}}^{EM} - {t_{ij}}^{Maxwell} \tag{5}$$

where

$$\begin{aligned} {t_{ij}}^{EM} &= P_i E_j - B_i M_j + \varepsilon_0 E_i E_j + \frac{1}{\mu_0} B_i B_j \\ &-\frac{1}{2}\left(\varepsilon_0 E^2 + \frac{1}{\mu_0} B_k B_k - 2 M_k B_k\right)\delta_{ij} \end{aligned} \tag{6}$$

$$\begin{aligned} {t_{ij}}^{Maxwell} &= \varepsilon_0 E_i E_j + \frac{1}{\mu_0} B_i B_j \\ &-\frac{1}{2}\left(\varepsilon_0 E^2 + \frac{1}{\mu_0} B^2 - 2 M_k B_k\right)\delta_{ij} \end{aligned} \tag{7}$$

where ε_0 is the vacuum permittivity.

In the ferromagnetic materials, the electricity current generally can be generated by the magnetic field. In these materials, the amount of the magnetic field due to the uniform electrical current applied in the direction of the *x*-axis in the rectangular plane can be obtained as

$$\boldsymbol{B}_J = \begin{cases} \mu_0 J_0 \dfrac{h}{2}\boldsymbol{j} & z > -\dfrac{h}{2} \\ -\mu_0 J_0 \dfrac{h}{2}\boldsymbol{j} & z < \dfrac{h}{2} \\ 0 & z = 0 \\ -\mu_0 J_0 z \boldsymbol{j} & -\dfrac{h}{2} < z < \dfrac{h}{2} \end{cases} \tag{8}$$

Therefore, the total magnetic field intensity vector inside the GSs, which is equal to the summation of the magnetic intensity applied to the GSs, $B_0 = B_0 \hat{k}$, and the magnetic intensity generated in the GSs due to the electric current, B_J, is obtained as follows

$$\boldsymbol{B} = \boldsymbol{B}_0 + \boldsymbol{B}_J = -(\mu_0 J_0 z)\boldsymbol{j} + B_0 \boldsymbol{k}, \quad -\frac{h}{2} < z < \frac{h}{2} \tag{9}$$

Using Eqs. (3) and (9) the resultant magnetization vector is obtained as

$$\boldsymbol{M} = \chi_m \boldsymbol{H} = \frac{\chi_m}{\mu}\boldsymbol{B} = \frac{\chi_m}{\mu}[-\mu_0 J_0 z \boldsymbol{j} + B_0 \boldsymbol{k}] \tag{10}$$

Considering the quasi static state for the problem under study, because the wavelength of electromagnetic waves is much longer than mechanical waves, it is $\sigma \dot{w} \times B = 0$ and as a result, the electrical current density is obtained as

$$\boldsymbol{J} = \nabla \times \boldsymbol{M} + \boldsymbol{\sigma}(\dot{\boldsymbol{w}} \times \boldsymbol{B} + \boldsymbol{E}) = J_0 \left(\frac{1+2\chi_m}{1+\chi_m}\right)\boldsymbol{i} \tag{11}$$

in which $\boldsymbol{\sigma}$ is the electrical conductivity tensor, $\boldsymbol{E}$ is the electric field intensity vector, and since there is no single charge, its value is zero.

2.2 Electromagnetic force and torque

Supposing that the GSs is fully conductive, the magnetic forces acting on the sheet can be obtained by substituting Eqs. (9) and (11) in Eq. (3), and then integrating along the sheet. Therefore, the components of the electromagnetic force acting on the plate due to the property of magnetization and passage of the current through the magnetic field is written as

$$\boldsymbol{F}^{EM} = -B_0 J_0 h \frac{1+2\chi_m}{1+\chi_m}\boldsymbol{j} \tag{12}$$

Since the magnetic traction vector at the bottom and the top of the GSs generates magnetic coupling, Eq. (13) is used to compute the magnetic torques

$$t_i = {t_{ij}}^{EM} n_j = \begin{bmatrix} {t_{xx}}^{EM} & {t_{xy}}^{EM} & {t_{xz}}^{EM} \\ {t_{yx}}^{EM} & {t_{yy}}^{EM} & {t_{yz}}^{EM} \\ {t_{zx}}^{EM} & {t_{zy}}^{EM} & {t_{zz}}^{EM} \end{bmatrix} \begin{bmatrix} n_x \\ n_y \\ n_z \end{bmatrix} = \begin{bmatrix} t_x \\ t_y \\ t_z \end{bmatrix} \tag{13}$$

in which n_j is the normal vector to the GSs, which is obtained as

$$\boldsymbol{n} = -\left(\frac{\partial w}{\partial x}\right)\boldsymbol{i} - \left(\frac{\partial w}{\partial y}\right)\boldsymbol{j} + \left(1 - \frac{1}{2}\left[\left(\frac{\partial w}{\partial x}\right)^2 + \left(\frac{\partial w}{\partial y}\right)^2\right]\right)\boldsymbol{k} \tag{14}$$

The electromagnetic traction forces at the bottom and top of the GSs causes the magnetic couplings. By calculating the tractions generated at top and bottom of the GSs by Eq. (13), the magnetic couplings created on the ferromagnetic GSs can be calculated as

$$C_x = {}^{top}t_y \frac{h}{2} + {}^{bottom}t_y \frac{h}{2}, C_y = {}^{top}t_x \frac{h}{2} + {}^{bottom}t_x \frac{h}{2} \tag{15}$$

2.3 Theory of nonlocal elasticity

In the nonlocal elasticity theory, the stress at any desired

point is a function of the strain field, and the relationship between strain and stress is written as

$$t_{ij}(x) = \iiint \alpha\left(\left|x^{'} - x\right|, \tau\right) C_{ijkl}\varepsilon_{ij}(x^{'})dv(x^{'}) \quad (16)$$

where t_{ij}, ε_{ij}, C_{ijkl}, $|x' - x|$ are the nonlocal stress tensor, the strain tensor, and the fourth-order elasticity tensor, the Euclidean form of distance, respectively. α is the nonlocal kernel function, which function as the internal characteristic size. According to Eringen's nonlocal elasticity theory

$$(1 - \mu\nabla^2)t_{ij} = C_{ijkl}\varepsilon_{ij} \quad (17)$$

where $\mu = (\sigma_0 l_i)^2$ and ∇^2 are the nonlocal parameter and the Laplacein operator. Using Eq. (17), the structural relationships are expressed as

$$(1 - \mu\nabla^2)\begin{Bmatrix} t_x \\ t_y \\ t_{xy} \end{Bmatrix} = \begin{bmatrix} \frac{E}{1-\nu^2} & \frac{\nu E}{1-\nu^2} & 0 \\ \frac{\nu E}{1-\nu^2} & \frac{E}{1-\nu^2} & 0 \\ 0 & 0 & G \end{bmatrix}\begin{Bmatrix} \varepsilon_x \\ \varepsilon_y \\ \gamma_{xy} \end{Bmatrix} \quad (18)$$

where G, E and ν are the shear modulus, Young modulus and Poisson ratio, respectively.

2.4 Equations of motion

In order to derive the equations governing the flexural vibrations, the classical plate theory and the von-Kármán nonlinear theory are used. Accordingly, plate displacement fields are given in terms of mid-plane deformations as

$$\begin{aligned} u_1(x,y,z,t) &= u(x,y,t) - z\frac{\partial w(x,y,t)}{\partial x}, \\ u_2(x,y,z,t) &= v(x,y,t) - z\frac{\partial w(x,y,t)}{\partial y}, \\ w(x,y,z,t) &= w(x,y,t) \end{aligned} \quad (19)$$

where, considering the coordinate system in the mid-plane of the GSs, *u*, *v* and *w* are the displacements components of the GSs center plane in the direction of the axes x, y and z, respectively. Therefore, the displacement-strain relationships are as

$$\varepsilon_x = e_x - z\chi_x \quad (20)$$

$$\varepsilon_y = e_y - z\chi_y \quad (21)$$

$$\varepsilon_{xy} = e_{xy} - z\chi_{xy} \quad (22)$$

where

$$\begin{aligned} e_x &= \frac{\partial u}{\partial x} + \frac{1}{2}\left(\frac{\partial w}{\partial x}\right)^2, \\ e_y &= \frac{\partial v}{\partial y} + \frac{1}{2}\left(\frac{\partial w}{\partial y}\right)^2, \\ e_{xy} &= \frac{1}{2}\left(\frac{\partial u}{\partial y} + \frac{\partial u}{\partial x} + \frac{\partial w}{\partial x}\frac{\partial w}{\partial y}\right) \end{aligned} \quad (23)$$

$$\chi_x = \frac{\partial^2 w}{\partial x^2}, \chi_y = \frac{\partial^2 w}{\partial y^2}, \chi_{xy} = \frac{\partial^2 w}{\partial x \partial y} \quad (24)$$

Furthermore, the stress tensor is obtained as

$$t_{ij} = {t_{ij}}^M + {t_{ij}}^E \quad (25)$$

where ${t_{ij}}^E$ and ${t_{ij}}^M$ are the electromagnetic stress tensor and mechanical stress tensor, respectively. By assuming the studied sheet to be isotropic and elastic (Maugin 2013)

$${t_{ij}}^M = C_{klij}\varepsilon_{kl}^M = \lambda\varepsilon_{kk}^M\delta_{ij} + 2G\varepsilon_{ij}^M \quad (26)$$

where $G = \frac{E}{2(1+\nu)}$ and $\lambda = \frac{E\nu}{(1-2\nu)(1+\nu)}$ are the Lamé constants. By using the electromagnetic and mechanical stress from Eq. (5), the total stress tensor is expressed as

$$t_{ij} = C_{klij}(\varepsilon_{kl}^M + \varepsilon_{kl}^E) - B_i M_j \quad (27)$$

where ${\varepsilon_{ij}}^M$ and ${\varepsilon_{ij}}^E$ are mechanical and electromagnetic strain tensors, respectively. Electromagnetic strains are small compared to elastic strains and can be neglected, therefore

$$\varepsilon_{ij} = \varepsilon_{kl}^M = \frac{1+\nu}{E}{t_{ij}}^M - \frac{\nu}{E}{t_{kk}}^M\delta_{ij} \quad (28)$$

Considering an element of the ferromagnetic sheet, the resultant shear forces and bending moments can be obtained as follows

$$\left(N_{xx}, N_{yy}, N_{xy}\right) = \int_{-\frac{h}{2}}^{\frac{h}{2}}\left(t_{xx}, t_{yy}, t_{xy}\right)dz, \quad (29)$$

$$\left(M_{xx}, M_{yy}, M_{xy}\right) = \int_{-\frac{h}{2}}^{\frac{h}{2}}\left(t_{xx}, t_{yy}, t_{xy}\right)zdz, \quad (30)$$

Considering the small size effect and the theory of nonlocal elasticity

$$\begin{aligned} &(1 - \mu\nabla^2)\begin{Bmatrix} N_{xx} \\ N_{yy} \\ N_{xy} \end{Bmatrix} \\ &= K\begin{bmatrix} 1 & \nu & 0 \\ \nu & 1 & 0 \\ 0 & 0 & 1-\nu \end{bmatrix}\begin{Bmatrix} \frac{\partial u}{\partial x} + \frac{1}{2}\left(\frac{\partial w}{\partial x}\right)^2 \\ \frac{\partial v}{\partial y} + \frac{1}{2}\left(\frac{\partial w}{\partial y}\right)^2 \\ \frac{1}{2}\left(\frac{\partial u}{\partial y} + \frac{\partial v}{\partial x} + \frac{\partial w}{\partial x}\frac{\partial w}{\partial y}\right) \end{Bmatrix} \end{aligned} \quad (31)$$

$$(1 - \mu\nabla^2)\begin{Bmatrix} M_{xx} \\ M_{yy} \\ M_{xy} \end{Bmatrix} = -D\begin{bmatrix} 1 & \nu & 0 \\ \nu & 1 & 0 \\ 0 & 0 & 1-\nu \end{bmatrix}\begin{Bmatrix} \frac{\partial^2 w}{\partial x^2} \\ \frac{\partial^2 w}{\partial y^2} \\ \frac{\partial^2 w}{\partial x \partial y} \end{Bmatrix} \quad (32)$$

where $K = \frac{Eh}{(1-\nu^2)}$ and $D = \frac{Eh^3}{[12(1-\nu^2)]}$.

Using the Hamilton's principle, the equations of motion can be expressed as

$$\frac{\partial N_{xx}}{\partial x} + \frac{\partial N_{yx}}{\partial y} + {t_x}^{EM} = m_0\frac{\partial^2 u}{\partial t^2} \quad (33)$$

$$\frac{\partial N_{xy}}{\partial x} + \frac{\partial N_{yy}}{\partial y} + \left({F_y}^{EM} + {t_y}^{EM}\right) = m_0\frac{\partial^2 v}{\partial t^2} \quad (34)$$

$$\begin{aligned}&\frac{\partial^2 M_{xx}}{\partial x^2}+2\frac{\partial^2 M_{xy}}{\partial x\partial y}+\frac{\partial^2 M_{yy}}{\partial y^2}\\&+\frac{\partial}{\partial x}\left(N_{xx}\frac{\partial w}{\partial x}+N_{xy}\frac{\partial w}{\partial y}\right)+\frac{\partial}{\partial y}\left(N_y\frac{\partial w}{\partial y}+N_{xy}\frac{\partial w}{\partial x}\right)\\&+{t_z}^{EM}+\frac{\partial C_y}{\partial x}+\frac{\partial C_x}{\partial y}+q(t)\\&=m_0\frac{\partial^2 w}{\partial t^2}-m_2\left(\frac{\partial^4 w}{\partial x^2\partial t^2}+\frac{\partial^4 w}{\partial y^2\partial t^2}\right)\end{aligned}\tag{35}$$

where $m_0=\int_{-\frac{h}{2}}^{\frac{h}{2}}\rho dz$ and $m_2=\int_{-\frac{h}{2}}^{\frac{h}{2}}\rho z^2 dz$. $\frac{\partial C_y}{\partial x}$ and $\frac{\partial C_x}{\partial y}$ are the magnetic coupling forces created by magnetic tractions, respectively, and ${t_z}^{EM}$ is the forces created by the magnetic tractions. It should be noted that this force component is created due to the presence of magnetic field and electrical current in the GSs, and this term has been not presented in the models reported in previous studies in this field. Using Eqs. (13), (15) and (27), the electromagnetic bending torque and the tractions resultant vector in Eqs. (33)-(35) is obtained as follows

$$\begin{aligned}&\frac{\partial C_y}{\partial x}=-\frac{h}{8\mu_0(\chi_m+1)}\{4B_0^2(2\chi_m^2-1)\\&+h^2J_0^2\mu_0^2(\chi_m+1)^2(2\chi_m-1)\}\left(\frac{\partial^2 w}{\partial x^2}\right)\end{aligned}\tag{36}$$

$$\begin{aligned}&t_z=t_z^{\text{top}}+t_z^{\text{bottom}}\\&=\frac{1}{8\mu_0(1+\chi_m)}\left\{4B_0^2\left[(10\chi_m^2-2\chi_m-1)\left(\frac{\partial w}{\partial x}\right)^2\right]\right.\\&+4B_0^2(4\chi_m+2)\frac{\partial w}{\partial x}\\&\left.-h^2J^2\mu_0^2(\chi_m+1)^2(2\chi_m-1)\left(\left(\frac{\partial w}{\partial y}\right)^2-2\frac{\partial w}{\partial x}\right)\right\}\end{aligned}\tag{37}$$

$$\begin{aligned}&t_x=t_x^{\text{top}}+t_x^{\text{bottom}}\\&=-\frac{1}{4\mu_0(1+\chi_m)}\left(h^2J^2\mu_0^2(1+\chi_m)^2(-1+2\chi_m)\right.\\&\left.+B_0^2(-4+8\chi_m^2)\right)\left(\frac{\partial w}{\partial x}\right)\end{aligned}\tag{38}$$

$$\begin{aligned}&t_y=t_y^{\text{top}}+t_y^{\text{bottom}}\\&=\frac{-1}{4\mu_0(1+\chi_m)}\left(h^2J^2\mu_0^2(1+\chi_m)^2(-1+2\chi_m)\right.\\&\left.+B_0^2(-4+8\chi_m^2)\right)\left(\frac{\partial w}{\partial y}\right)\end{aligned}\tag{39}$$

Assuming that the motion along the *z*-axis is dominant, with acceptable accuracy, it can be assumed that $\frac{\partial^2 u}{\partial t^2}=\frac{\partial^2 v}{\partial t^2}=0$. Accordingly, substituting Eqs. (31) and (32) in Eqs. (33)-(35), the nonlinear differential equations governing the vibrations of ferromagnetic GSs under the influence of magnetic forces in terms of the displacement fields are obtained as

$$\begin{aligned}&K\left(\frac{\partial^2 u}{\partial x^2}+\frac{\partial w}{\partial x}\frac{\partial^2 w}{\partial x^2}+\nu\left(\frac{\partial^2 v}{\partial x\partial y}+\frac{\partial w}{\partial y}\frac{\partial^2 w}{\partial x\partial y}\right)\right)\\&+\frac{K(1-\nu)}{2}\left(\frac{\partial^2 u}{\partial y^2}+\frac{\partial^2 v}{\partial x\partial y}+\frac{\partial w}{\partial x}\frac{\partial^2 w}{\partial y^2}+\frac{\partial w}{\partial y}\frac{\partial^2 w}{\partial x\partial y}\right)\\&+(1-\mu\nabla^2){t_x}^{EM}=0\end{aligned}\tag{40}$$

$$\begin{aligned}&K\left(\frac{\partial^2 v}{\partial y^2}+\frac{\partial w}{\partial y}\frac{\partial^2 w}{\partial y^2}+\nu\left(\frac{\partial^2 u}{\partial x\partial y}+\frac{\partial w}{\partial x}\frac{\partial^2 w}{\partial x\partial y}\right)\right)\\&+\frac{K(1-\nu)}{2}\left(\frac{\partial^2 v}{\partial x^2}+\frac{\partial^2 u}{\partial x\partial y}+\frac{\partial w}{\partial y}\frac{\partial^2 w}{\partial x^2}+\frac{\partial w}{\partial x}\frac{\partial^2 w}{\partial x\partial y}\right)\\&+(1-\mu\nabla^2)\left({F_y}^{EM}+{t_y}^{EM}\right)=0\end{aligned}\tag{41}$$

$$\begin{aligned}&D\left(\frac{\partial^4 w}{\partial x^4}+2\frac{\partial^2 w}{\partial x^2\partial y^2}+\frac{\partial^4 w}{\partial y^4}\right)\\&=(1-\mu\nabla^2)\left({t_z}^{EM}+\frac{\partial C_y}{\partial x}+\frac{\partial C_x}{\partial y}+q(t)\right)+N_x\frac{\partial^2 w}{\partial x^2}\\&+2N_{xy}\frac{\partial^2 w}{\partial x\partial y}+N_y\frac{\partial^2 w}{\partial y^2}-(1-\mu\nabla^2){t_x}^{EM}\frac{\partial w}{\partial x}\\&-(1-\mu\nabla^2)\left({F_y}^{EM}+{t_y}^{EM}\right)\frac{\partial w}{\partial y}-(1-\mu\nabla^2)m_0\frac{\partial^2 w}{\partial t^2}\\&+(1-\mu\nabla^2)m_2\left(\frac{\partial^4 w}{\partial x^2\partial t^2}+\frac{\partial^4 w}{\partial y^2\partial t^2}\right)\end{aligned}\tag{42}$$

3. Solving the governing equations

In order to solve the differential governing equations which are nonlinear coupled equations, the Galerkin decomposition technique is established. Considering the simply supported boundary conditions, the displacement fields are expressed as (Amabili 2006)

$$\begin{aligned}&u(x,y,t)=U(t)\,cos(\alpha x)\,sin(\beta y)\\&v(x,y,t)=V(t)\,sin(\alpha x)\,cos(\beta y)\\&w(x,y,t)=W(t)\,sin(\alpha x)\,sin(\beta y)\end{aligned}\tag{43}$$

where the functions $U(t)$, $V(t)$ and $W(t)$ are generalized coordinates. By applying the Galerkin method, $U(t)$ and $V(t)$ are obtained from Eqs. (40) and (41) in terms of $W(t)$. By substituting this function in Eq. (42), the nonlinear differential equation governing the time part of the deflection for the ferromagnetic nanosheet, which is a second-order differential equation, is obtained as follows

$$\frac{d^2W}{\partial t^2}+a_1W(t)+a_2W(t)^2+a_3W(t)^3=\lambda\,sin(\omega t)\tag{44}$$

where the coefficients α_i are the constants from the stiffness matrices components and the sheet geometric derivatives. The spectrum analysis is conducted by short-time Fourier transform (STFT). The short-time Fourier transform allows to perform time-frequency analysis and obtaining the frequencies of nonlinear systems. Despite the FFT method, STFT method breaks up the signal in time domain to a number of signals of shorter duration, then transforms each signal to frequency domain (Allen and Rabiner 1977). For this purpose, after obtaining the numerical solution of Eq. (44) by Runge–Kutta methods, the time response of the system is extracted, and by applying the STFT, the spectrum response of the system is obtained in the frequency domain. Since, the frequency

curve peaks represent the frequencies in the time response, it can be used to extract the nonlinear frequency values of the system for various parameters. Then, by using the numerical solution of Eq. (44), the effect of various parameters on the dynamic response and vibration characteristics of electrically conductive sheets exposed to magnetic field are studied.

4. Numerical results

In this section, the vibrational behavior of GSs carrying electric current and located in magnetic field is investigated. First, the results are validated, and then the effect of different parameters on linear and nonlinear natural frequencies is studied. Considering linear terms and eliminating nonlinear terms from the GSs equations of motion, the linear natural frequencies of the system can be obtained. In Table 1, the obtained natural frequencies of local and nonlocal models for square GSs are compared with the reference results (Wang *et al.* 2015). According to this table, it can be seen that the results obtained from this study are completely consistent with the reference results (Wang *et al.* 2015), and this shows the high accuracy of the current method. Also, in Table 2, the natural frequency of a simply supported monolayer GSs (E = 1.02TPa, h = 0.33 nm, ρ = 2300 kg / m^3, $a = b$ = 10 nm) have been compared with the exact solution presented in Refs. (Pradhan and Phadikar 2009, Kitipornchai *et al.* 2005). As it can be seen, the numerical results obtained from this study have acceptable consistency with the solutions obtained from the exact solution.

In the next, effect of various parameters on the linear and nonlinear natural frequencies of the system is investigated. The numerical values used to extract the results are given in Table 3. Also, dimensionless parameters, including dimensionless linear natural frequency Ω_L, dimensionless nonlinear natural frequency Ω_N, dimensionless magnetic field intensity β_B, and dimensionless electric current β_J are defined as follows

$$\Omega_L = \omega \frac{b^2}{\pi^2}\sqrt{\frac{m_0}{D}}, \beta_B = \sqrt{\frac{B}{\left(\frac{h^3}{\mu_0 D}\right)^2}}, \beta_J = \sqrt{\frac{\mu_0 h^5}{D}} J \qquad (45)$$

Fig. 2 depicts the effect of the electrical current and magnetic field intensity on dimensionless linear natural frequency of the GSs for different values of μ. Based on the results, it is observed that the magnetic field increases the linear natural frequency of the GSs, and the amount of this increase intensifies with increasing the magnetic field. As can be seen, for values of β_B less than 18, the magnetic fields have little effect on increasing the natural frequency, and in these areas the effect of the magnetic field can be ignored. In contrast, as β_B increases, the natural frequency of the system increases sharply. As an instance, for β_B = 40 natural frequency increases by about 5 times the GSs frequency in the absence of magnetic field. In the case of electric current, the same behavior is observed, with the difference that the effect of electric current on the increase of natural frequency is relatively less than the effect of

Table 1 Comparison of frequency ratios for square nanosheets

μ	$\frac{\omega_1^{non}}{\omega_1^{loc}}$	
	Ref. (Wang *et al.* 2015)	Present results
0	1.0000	0.9999
0.5	0.9762	0.9762
1.0	0.9139	0.9139
1.5	0.8321	0.8321

Table 2 Comparison of the natural frequencies of the simply supported GSs with exact solution

	μ = 0			μ = 1	
	Present result	Exact[a]	Exact[b]	Present result	Exact[b]
ω_1 (THz)	10.5546	10.5586	10.5586	9.67153	9.67400
ω_2 (THz)	26.4761	26.4753	26.4753	21.6223	21.6246
ω_3 (THz)	52.7283	52.7295	52.7295	37.4056	37.4075

Table 3 Numerical values used in this study

Parameter	Value	Parameter	Value
a (nm)	10	ν	0.186
b (nm)	10	μ (nm)	1.5
h (nm)	1.5	μ_0 (H/m)	$4\pi \times 10^{-7}$
ρ (kg/m^3)	1062.5	χ_m	15
E (TPa)	1.01		

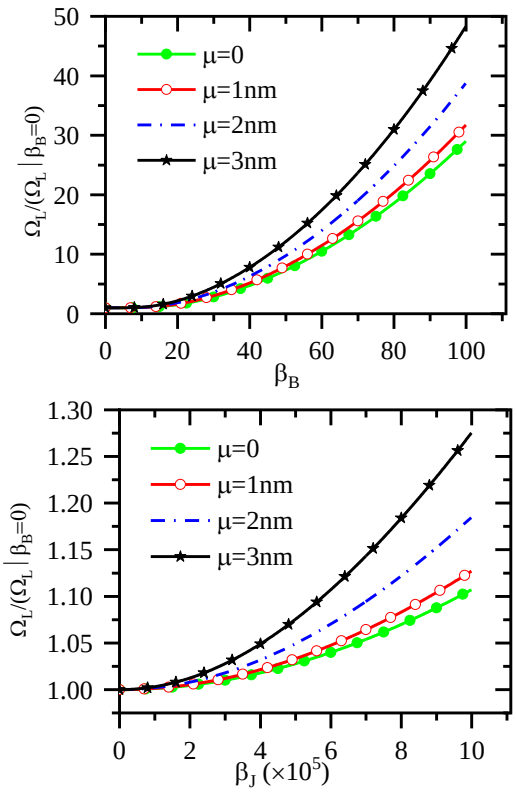

Fig. 2 Influence of electrical current and magnetic field intensity on dimensionless linear natural frequency of the GSs for different values of μ

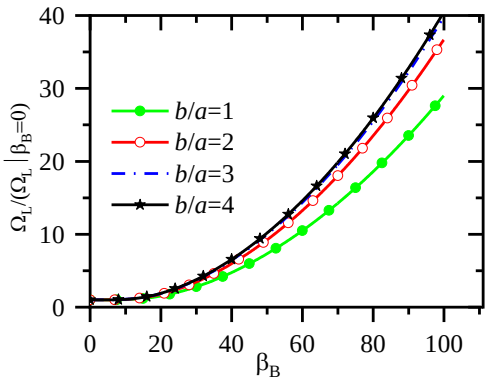

Fig. 3 Effect of aspect ratio on natural frequency of the simply supported GSs

magnetic field. Fig. 3 shows the frequency ratio changes in terms of β_B for different aspect ratio values. As can be seen, the frequency ratio increases with increase in aspect ratio, and converges to a certain value. Based on these results, it is observed that values of aspect ratio greater than 3 have no effect on frequency increase.

In the following, the behavior of nonlinear vibrations of the simply supported GSs is investigated. The dynamic response along with the frequency response curves and the phase curve of the GSs for different values of β_B (i.e., 0.01, 0.02 and 0.023) are shown in Fig. 4. As shown, for very small values of β_B, the behavior of the system is linear, and the oscillations frequency is approximately equal to the normal frequency of the linear system. In contrast, with increasing β_B, the coefficient of nonlinear terms becomes larger, and the nonlinear behavior of the system is amplified, which is clearly visible due to the creation of second- and third-order super-harmonics in the frequency function of Fig. 4(b). Fig. 4(b) shows that for β_B = 0.02 and β_B = 0.023, the resonance frequency of the system decreases by about 12% and 52%, respectively, compared to the normal frequency of the GSs in the absence of magnetic field. Considering that the magnetic field reduces the natural frequency, it can be said that the magnetic field causes the softening behavior, and as a result, excessive increase of the magnetic field can cause instability in the system. This can be seen in Fig. 5, where the dynamic response of the system for β_B = 0.025 is demonstrated. As shown, for the critical β_B = 0.025, the amplitude of the system vibrations increases over time, and tends towards very large values. Due to the fact that in such conditions, the motion of the system is oscillating, the intensity of the critical magnetic field will cause dynamic instability.

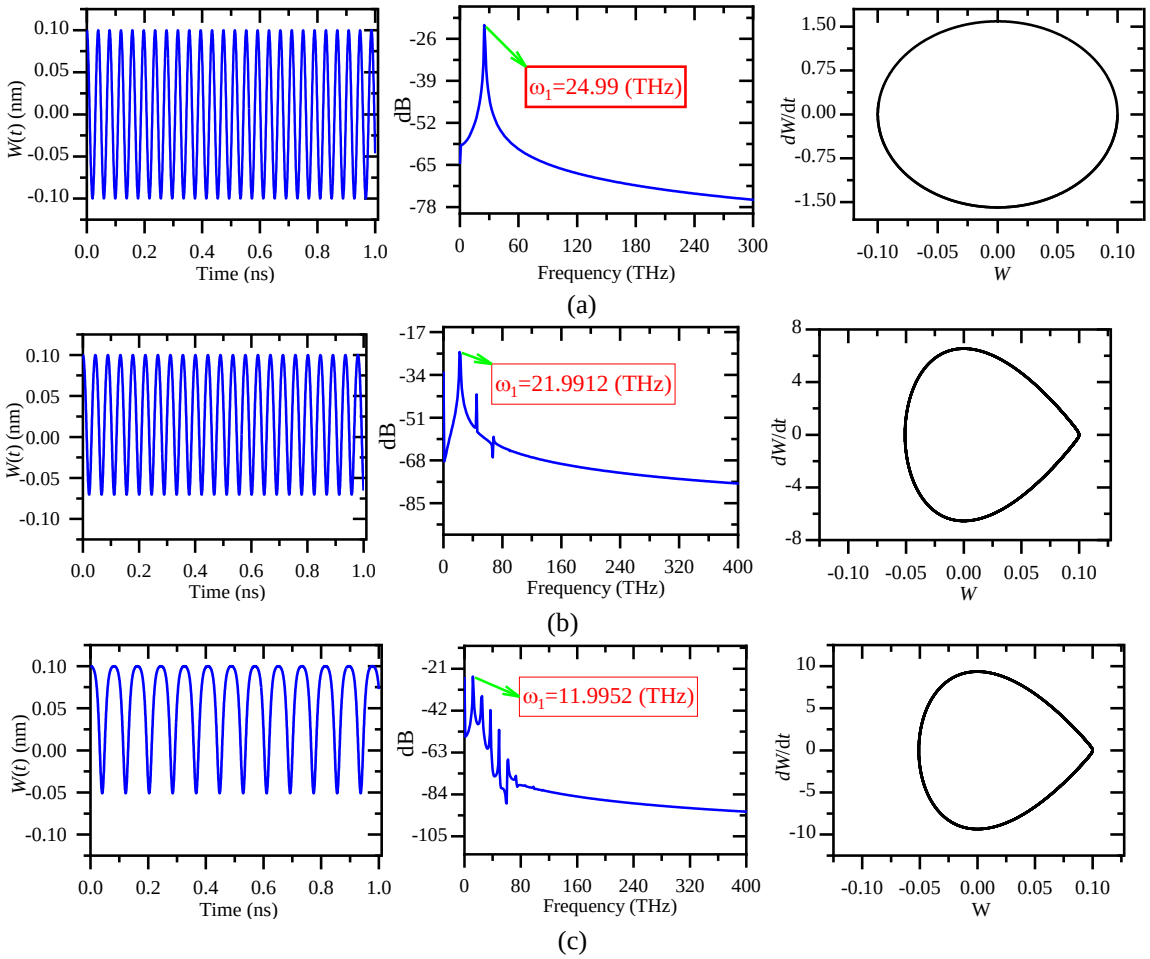

Fig. 4 Dynamic response, frequency response curve and phase curve of monolayer GSs for different values of β_B (a) = 0.01; (b) 0.02; and (c) 0.023

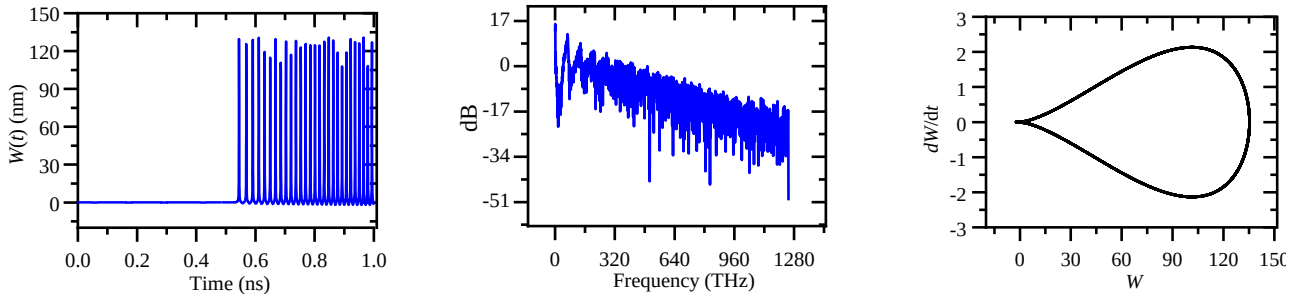

(a) (b) (c)

Fig. 5 (a) Dynamic response; (b) frequency response curve; and (c) phase curve of monolayer GSs for critical β_B equal to 0.025

Table 4 Influence of magnetic field intensity on nonlinear resonance frequency (THz) of simply supported GSs for b = 10 nm

β_B	μ = 0			μ = 1 nm		
	Ω_L	Ω_N	$\frac{\Omega_N}{\Omega_L}$	Ω_L	Ω_N	$\frac{\Omega_N}{\Omega_L}$
0	27.71	27.45	0.99	25.32	25.42	1.00
5	27.77	8.34	0.30	25.41	9.21	0.36
10	28.86	5.28	0.18	26.57	6.04	0.23
15	33.10	3.72	0.11	31.13	4.26	0.14
20	42.48	1.09	0.03	40.96	1.83	0.04

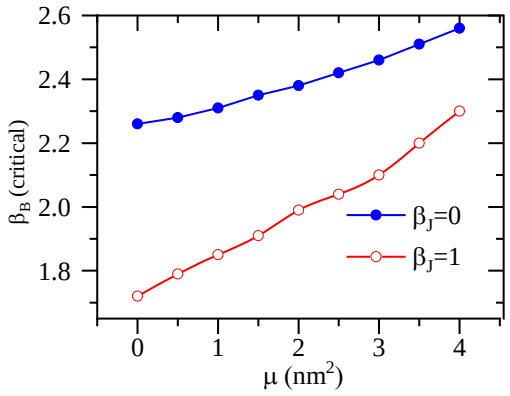

Fig. 6 Effect of the nonlocal parameter on critical value of the applied magnetic field intensity

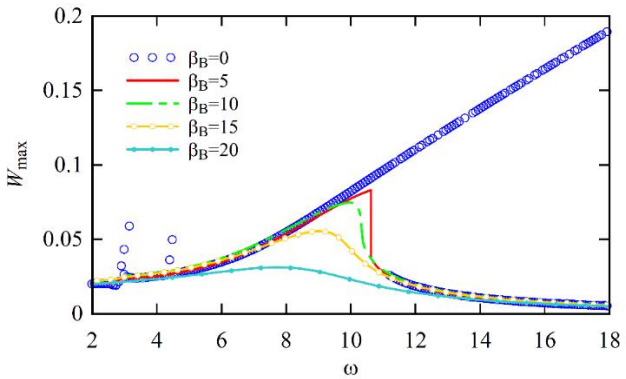

Fig. 7 Frequency-response curve of GSs oscillations in terms of external harmonic force frequency for different values of β_B

Table 4 shows the influence of the magnetic field intensity on nonlinear resonance frequency of monolayer simply supported GSs. An interesting result that can be seen according to the results of this table is that linear frequencies increases with increase in magnetic field intensity, while the nonlinear frequency decreases significantly. The reason for this behavior is that with increasing the magnetic field intensity, the effect of geometrical nonlinearity becomes more severe, and the ratio of nonlinear frequency to linear frequency decreases sharply. Based on these results, it can be concluded that with increasing the magnetic field intensity, the coefficient of nonlinear terms increases, and as a result, in larger amounts of magnetic field intensity, geometric nonlinear effects should be considered to achieve accurate and realistic results. Since, the use of linear theory does not predict the instability behavior of these systems, using this theory to predict the dynamic behavior of GSs located in a magnetic field will lead to erroneous results. Another interesting result that can be seen from Table 4 is that the effect of nonlocal parameter on natural frequency is quite different in both linear and nonlinear theories. Increasing the nonlocal parameter increases the linear natural frequency, while decreasing the nonlinear natural frequency. It can be stated that in general, the equivalent stiffness of the structure can be simulated using a linear spring and a nonlinear spring. According to the effect of magnetic field and nonlocal parameter, it can be stated that the magnetic field causes softening behavior, while nonlocal parameter causes hardening behavior in nonlinear model.

Fig. 6 shows effect of the nonlocal parameter on critical value of the magnetic field intensity of the GSs. Increasing the nonlocal parameter, the intensity of the critical magnetic field also increases. Based on this, it can be stated that the nonlocal parameter increases the stability range of the GSs by increasing the equivalent stiffness of the structure. As an example, for $\beta_J = 0$, an increase of μ from zero to 2, increases β_B by about 6%. In addition, it is observed that the electrical current also reduces the intensity of the critical magnetic field. Increasing β_J from zero to 1 decreases the critical β_B by about 34%.

In order to investigate the behavior of electro-magnetic coupling of GSs, which carries electric current, and is exposed to magnetic field and external harmonic force, the frequency response of the system in steady state has been extracted. Fig. 7 shows the maximum amplitude of GSs

oscillations in terms of external harmonic force frequency for different values of β_B. As the results show, due to the nonlinear behavior in the system in certain areas of the excitation frequency, the jump phenomenon occurs. In the absence of a magnetic field, it occurs with increasing frequency of excitation of resonant regions in the system. Resonances are created in the vicinity of 9 and 11, and when this parameter reaches to 10.05, the jump phenomenon occurs, and the behavior of the system becomes unstable. Another conclusion that can be seen from Fig. 7 is that the magnetic field has significant effect on the frequency-amplitude curve of these systems. By increasing the parameter β_B, the jump phenomenon is removed from the system behavior. For $\beta_B = 5$, the jump phenomenon is observed in the region of $\omega = 10.6$ and, with increasing the value of this parameter, the maximum amplitude of fluctuations is sharply reduced, and resonant regions are not observed in the dynamic behavior of the system.

5. Conclusions

In the present work, the vibration behavior of simply supported graphene nanosheets was studied by considering the interactions between the displacement fields and magnetic field created forces. Considering the influences of the magnetic tractions created by electrical and eddy currents, new mathematical relationships were presented for the interactions between electromagnetic fields with ferromagnetic materials. The nonlinear governing motion equations were extracted using the nonlocal classical plate theory considering von Kármán nonlinear theory, and then discretized using the Galerkin method. After solving the equations numerically, effect of different parameters on linear and nonlinear frequencies was studied. A summary of the current study results is as follows:

- The magnetic field increases the linear natural frequency, and decreases the nonlinear frequencies of the GSs. These changes are intensified by increasing the magnetic field.
- The interaction between magnetic field and electrical current leads to nonlinear behavior of the structure, and has softening effect, which reduces natural frequencies, and creates instability.
- The critical magnetic field increases with increasing nonlocal parameter and decreases with increasing the electric current.
- The vibrational behavior of GSs located in the magnetic field cannot be analyzed by linear theories. In order to achieve acceptable results, the effects of geometric nonlinearity should be considered in the equations.

References

Ajri, M. and Seyyed Fakhrabadi, M.M. (2018), "Nonlinear free vibration of viscoelastic nanoplates based on modified couple stress theory", *J. Comput. Appl. Mech.*, **49**(1), 44-53. http://doi.org/10.22059/JCAMECH.2018.228477.129.

Ajri, M., Fakhrabadi, M.M.S. and Rastgoo, A. (2018), "Analytical solution for nonlinear dynamic behavior of viscoelastic nanoplates modeled by consistent couple stress theory", *Lat. Am. J. Solid. Struct.*, **15**, 78-90. http://doi.org/10.1590/1679-78254918.

Al-Furjan, M., Dehini, R., Paknahad, M., Habibi, M. and Safarpour, H. (2021), "On the nonlinear dynamics of the multi-scale hybrid nanocomposite-reinforced annular plate under hygro-thermal environment", *Arch. Civ. Mech. Eng.*, **21**(1), 1-25. https://doi.org/10.1007/s43452-020-00151-w.

Allahyari, E., Asgari, M. and Jafari, A.A. (2020), "Nonlinear size-dependent vibration behavior of graphene nanoplate considering surfaces effects using a multiple-scale technique", *Mech. Adv. Mater. Struct.*, **27**(9), 697-706. https://doi.org/10.1080/15376494.2018.1494870.

Allen, J.B. and Rabiner, L.R. (1977), "A unified approach to short-time Fourier analysis and synthesis", *Proceedings of the IEEE*, **65**(11), 1558-1564.

Amabili, M. (2006), "Theory and experiments for large-amplitude vibrations of rectangular plates with geometric imperfections", *J. Sound Vib.*, **291**(3-5), 539-565. https://doi.org/10.1016/j.jsv.2005.06.007

Ansari, R. and Ajori, S. (2015), "Vibrational characteristics of diethyltoluenediamines (DETDA) functionalized carbon nanotubes using molecular dynamics simulations", *Physica B*, **459**, 58-61. https://doi.org/10.1016/j.physb.2014.11.101.

Ansari, R., Ajori, S. and Darvizeh, M. (2015), "Vibration characteristics of single- and double-walled carbon nanotubes functionalized with amide and amine groups", *Physica B*, **462**, 8-14. https://doi.org/10.1016/j.physb.2015.01.003.

Ansari, R., Sadeghi, F. and Darvizeh, M. (2016), "Continuum study on the oscillatory characteristics of carbon nanocones inside single-walled carbon nanotubes", *Physica B*, **482**, 28-37. https://doi.org/10.1016/j.physb.2015.11.028.

Asadi, E., Askari, H., Behrad Khamesee, M. and Khajepour, A. (2017), "High frequency nano electromagnetic self-powered sensor: Concept, modelling and analysis", *Measurement*, **107**, 31-40. https://doi.org/10.1016/j.measurement.2017.04.019.

Assadi, A. (2013), "Size dependent forced vibration of nanoplates with consideration of surface effects", *Appl. Math. Model.*, **37**(5), 3575-3588. https://doi.org/10.1016/j.apm.2012.07.049.

Attar, F., Khordad, R., Zarifi, A. and Modabberasl, A. (2021), "Application of nonlocal modified couple stress to study of functionally graded piezoelectric plates", *Physica B*, **600**, 412623. https://doi.org/10.1016/j.physb.2020.412623.

Aydogdu, M., Arda, M. and Filiz, S. (2018), "Vibration of axially functionally graded nano rods and beams with a variable nonlocal parameter", *Adv. Nano Res., Int. J.*, **6**(3), 257-278. http://doi.org/10.12989/anr.2018.6.3.257.

Barretta, R., Faghidian, S.A. and Marotti de Sciarra, F. (2019), "Stress-driven nonlocal integral elasticity for axisymmetric nano-plates", *Int. J. Eng. Sci.*, **136**, 38-52. https://doi.org/10.1016/j.ijengsci.2019.01.003.

Basutkar, R. (2019), "Analytical modelling of a nanoscale series-connected bimorph piezoelectric energy harvester incorporating the flexoelectric effect", *Int. J. Eng. Sci.*, **139**, 42-61. https://doi.org/10.1016/j.ijengsci.2019.01.007.

Bendaho, B., Belabed, Z., Bourada, M., Benatta, M.A., Bourada, F. and Tounsi, A. (2019), "Assessment of new 2D and quasi-3D Nonlocal theories for free vibration analysis of size-dependent functionally graded (FG) nanoplates", *Adv. Nano Res., Int. J.*, **7**(4), 277-292. https://doi.org/10.12989/anr.2019.7.4.277.

Bouadi, A., Bousahla, A.A., Houari, M.S.A., Heireche, H. and Tounsi, A. (2018), "A new nonlocal HSDT for analysis of stability of single layer graphene sheet", *Adv. Nano Res., Int. J.*, **6**(2), 147-162. http://doi.org/10.12989/anr.2018.6.2.147.

Chandra, Y., Mukhopadhyay, T. and Adhikari, S. (2020), "Size-dependent dynamic characteristics of graphene based multi-layer nano hetero-structures", *Nanotechnology*, **31**(14), 145705.

Chen, L., Pan, S., Fei, Y., Zhang, W. and Yang, F. (2019), "Theoretical study of micro/nano-scale bistable plate for flexoelectric energy harvesting", *Appl. Phys. A*, **125**(4), 242-267. https://doi.org/10.1007/s00339-019-2539-3.

Chung, T. (2007), *General Continuum Mechanics*, Cambridge University Press.

Cicek, S. and Nadaroglu, H. (2015), "The use of nanotechnology in the agriculture", *Adv. Nano Res., Int. J.*, **3**(4), 207-231. http://doi.org/10.12989/anr.2015.3.4.207.

Di Sia, P. (2013), "A new theoretical Model for the dynamical Analysis of Nano-Bio-Structures", *Adv. Nano Res., Int. J.*, **1**(1), 29-42. http://doi.org/10.12989/anr.2013.1.1.029.

Ebrahimi, F., Babaei, R. and Shaghaghi, G.R. (2018), "Vibration analysis thermally affected viscoelastic nanosensors subjected to linear varying loads", *Adv. Nano Res., Int. J.*, **6**(4), 399-412. http://doi.org/10.12989/anr.2018.6.4.399.

Fakhrabadi, M.M.S., Rastgoo, A. and Ahmadian, M.T. (2015), "Application of electrostatically actuated carbon nanotubes in nanofluidic and bio-nanofluidic sensors and actuators", *Measurement*, **73**, 127-136. https://doi.org/10.1016/j.measurement.2015.05.009.

Farajpour, A., Mohammadi, M., Shahidi, A. and Mahzoon, M. (2011), "Axisymmetric buckling of the circular graphene sheets with the nonlocal continuum plate model", *Physica E*, **43**(10), 1820-1825. https://doi.org/10.1016/j.physe.2011.06.018.

Fazelzadeh, S.A. and Ghavanloo, E. (2014), "Nanoscale mass sensing based on vibration of single-layered graphene sheet in thermal environments", *Acta Mechanica Sinica*, **30**(1), 84-91. https://doi.org/10.1007/s10409-013-0102-6.

Ghadiri, M., Rajabpour, A. and Akbarshahi, A. (2018), "Non-linear vibration and resonance analysis of graphene sheet subjected to moving load on a visco-Pasternak foundation under thermo-magnetic-mechanical loads: An analytical and simulation study", *Measurement*, **124**, 103-119. https://doi.org/10.1016/j.measurement.2018.04.007.

Ghannadpour, S. and Moradi, F. (2019), "Nonlocal nonlinear analysis of nano-graphene sheets under compression using semi-Galerkin technique", *Adv. Nano Res., Int. J.*, **7**(5), 311-324. http://doi.org/10.12989/anr.2019.7.5.311.

Ghorbanpour Arani, A., Maboudi, M., Ghorbanpour Arani, A. and Amir, S. (2013), "2D-magnetic field and biaxiall in-plane pre-load effects on the vibration of double bonded orthotropic graphene sheets", *J. Solid Mech.*, **5**(2), 193-205.

Kachapi, S.H.H. (2020), "Nonlinear and nonclassical vibration analysis of double walled piezoelectric cylindrical nanoshell", *Adv. Nano Res., Int. J.*, **9**(4), 277-294. http://doi.org/10.12989/anr.2020.9.4.277.

Karami, B. and Karami, S. (2019), "Buckling analysis of nanoplate-type temperature-dependent heterogeneous materials", *Adv. Nano Res., Int. J.*, **7**(1), 51-65. http://doi.org/10.12989/anr.2019.7.1.051.

Kheradmandan, H. and Barati, F. (2017), "Modeling width of Weld in SAW with Adding Nano Material", *J. Res. Sci. Eng. Technol.*, **5**(2), 1-7.

Khodashenas, B. (2015), "Nitrate reductase enzyme in Escherichia coli and its relationship with the synthesis of silver nanoparticles", *UCT J. Res. Sci. Eng. Technol.*, **3**(1), 26-32.

Kitipornchai, S., He, X. and Liew, K. (2005), "Continuum model for the vibration of multilayered graphene sheets", *Phys. Rev. B*, **72**(7), 89-97. https://doi.org/10.1103/PhysRevB.72.075443.

Kumar, T.P., Narendar, S. and Gopalakrishnan, S. (2013), "Thermal vibration analysis of monolayer graphene embedded in elastic medium based on nonlocal continuum mechanics", *Compos. Struct.*, **100**, 332-342. https://doi.org/10.1016/j.compstruct.2012.12.039.

Le, K.Q. (2020), "Electromagnetic modeling of excited-state dynamics in the vicinity of metallic nanostructures", *Physica B*, **45**, 81-97. https://doi.org/10.1016/j.physb.2020.412381.

Lu, T.-F., Fan, Y. and Morita, T. (2019), "An investigation of piezoelectric actuator high speed operation for self-sensing", *Measurement*, **136**, 105-115. https://doi.org/10.1016/j.measurement.2018.12.055.

Maugin, G.A. (2013), "Continuum mechanics and electromagnetism", In: *Continuum Mechanics Through the Twentieth Century*, 199-221. Springer, Dordrecht. https://doi.org/10.1007/978-94-007-6353-1_12.

Mehrez, S., Karati, S.A., Dolat Abadi, P.T., Shah, S., Azam, S., Khorami, M. and Assilzadeh, H. (2020), "Nonlocal dynamic modeling of mass sensors consisting of graphene sheets based on strain gradient theory", *Adv. Nano Res., Int. J.*, **9**(4), 221-235. https://doi.org/10.12989/anr.2020.9.4.221.

Mohammadi, M., Farajpour, A., Moradi, A. and Ghayour, M. (2014), "Shear buckling of orthotropic rectangular graphene sheet embedded in an elastic medium in thermal environment", *Compos. Part B-Eng.*, **56**, 629-637. https://doi.org/10.1016/j.compositesb.2013.08.060.

Mohammadian, M., Abolbashari, M.H. and Hosseini, S.M. (2019), "Axial vibration of hetero-junction CNTs mass nanosensors by considering the effects of small scale and connecting region: An analytical solution", *Physica B*, **553**, 137-150. https://doi.org/10.1016/j.physb.2018.10.044.

Murmu, T. and Pradhan, S. (2009), "Vibration analysis of nano-single-layered graphene sheets embedded in elastic medium based on nonlocal elasticity theory", *J. Appl. Phys.*, **105**(6), 56-87. https://doi.org/10.1063/1.3091292.

Naderi, A. and Saidi, A.R. (2014), "Nonlocal postbuckling analysis of graphene sheets in a nonlinear polymer medium", *Int. J. Eng. Sci.*, **81**, 49-65. https://doi.org/10.1016/j.ijengsci.2014.04.004.

Ponmozhi, J., Frias, C., Marques, T. and Frazão, O. (2012), "Smart sensors/actuators for biomedical applications: Review", *Measurement*, **45**(7), 1675-1688. https://doi.org/10.1016/j.measurement.2012.02.006.

Pradhan, S. (2009), "Buckling of single layer graphene sheet based on nonlocal elasticity and higher order shear deformation theory", *Phys. Lett. A*, **373**(45), 4182-4188. https://doi.org/10.1016/j.physleta.2009.09.021.

Pradhan, S. and Phadikar, J. (2009), "Nonlocal elasticity theory for vibration of nanoplates", *J. Sound Vib.*, **325**(1-2), 206-223.

Rezaee, M. and Maleki, V.A. (2015), "An analytical solution for vibration analysis of carbon nanotube conveying viscose fluid embedded in visco-elastic medium", *Proceedings of the Institution of Mechanical Engineers, Part C: J. Mech. Eng. Sci.*, **229**(4), 644-650. https://doi.org/10.1177/0954406214538011.

Rezaei, A., Kamali, B. and Kamali, A.R. (2020), "Correlation between morphological, structural and electrical properties of graphite and exfoliated graphene nanostructures", *Measurement*, **150**, 76-89. https://doi.org/10.1016/j.measurement.2019.107087.

Salimi, M., Khoddam, K., Morakkabatchy, D. and Pornadem, M. (2015), "Optimization of carbon nano tube field-effect transistors (CNTFET) and compare them to CMOS silicon", *J. Res. Sci. Eng. Technol.*, **3**(4), 10-16.

Salmani, R., Gholami, R., Ansari, R. and Fakhraie, M. (2021), "Analytical investigation on the nonlinear postbuckling of functionally graded porous cylindrical shells reinforced with graphene nanoplatelets", *Eur. Phys. J. Plus*, **136**(1), 1-19. https://doi.org/10.1140/epjp/s13360-020-01009-z.

Samaei, A., Abbasion, S. and Mirsayar, M. (2011), "Buckling analysis of a single-layer graphene sheet embedded in an elastic medium based on nonlocal Mindlin plate theory", *Mech. Res. Commun.*, **38**(7), 481-485. https://doi.org/10.1016/j.mechrescom.2011.06.003.

Saremi, M., Saremi, M., Niazi, H. and Goharrizi, A.Y. (2013),

"Modeling of lightly doped drain and source graphene nanoribbon field effect transistors", *Superlatt. Microstruct.*, **60**, 67-72. https://doi.org/10.1016/j.spmi.2013.04.013.

Shafiei, Z., Sarrami-Foroushani, S., Azhari, F. and Azhari, M. (2020), "Application of modified couple-stress theory to stability and free vibration analysis of single and multi-layered graphene sheets", *Aerosp. Sci. Technol.*, **98**, 105-122. https://doi.org/10.1016/j.ast.2019.105652.

Shen, H. and Huang, X. (2007), "Nonlinear vibration and transient analysis of hybrid laminated plates", *Anal. Des. Plated Struct.*, **56**, 376-421. https://doi.org/10.1533/9781845692292.376.

Shen, L., Shen, H.-S. and Zhang, C.-L. (2010), "Nonlocal plate model for nonlinear vibration of single layer graphene sheets in thermal environments", *Comp. Mater. Sci.*, **48**(3), 680-685. https://doi.org/10.1016/j.commatsci.2010.03.006.

Singh, P.P. and Azam, M.S. (2020), "Free vibration and buckling analysis of elastically supported transversely inhomogeneous functionally graded nanoplate in thermal environment using Rayleigh–Ritz method", *J. Vib. Control*, **56**, 67-89. https://doi.org/10.1177/1077546320966932.

Tao, C. and Dai, T. (2020), "Isogeometric analysis for size-dependent nonlinear free vibration of graphene platelet reinforced laminated annular sector microplates", *Eur. J. Mech. A-Solid.*, **45**, 92-106. https://doi.org/10.1016/j.euromechsol.2020.104171.

Tezerjani, M.D., Benvidi, A., Dehghani Firouzabadi, A., Mazloum-Ardakani, M. and Akbari, A. (2017), "Epinephrine electrochemical sensor based on a carbon paste electrode modified with hydroquinone derivative and graphene oxide nano-sheets: Simultaneous determination of epinephrine, acetaminophen and dopamine", *Measurement*, **101**, 183-189. https://doi.org/10.1016/j.measurement.2017.01.029.

Trimarco, C. and Maugin, G.A. (2001), "Material mechanics of electromagnetic solids", In: *Configurational Mechanics of Materials*, 129-171. Springer, Vienna, Austria. https://doi.org/10.1007/978-3-7091-2576-2_3.

Umar, A., Ibrahim, A.A., Nakate, U.T., Albargi, H., Alsaiari, M.A., Ahmed, F., Alharthi, F.A., Ali Alghamdi, A. and Al-Zaqri, N. (2021), "Fabrication and characterization of CuO nanoplates based sensor device for ethanol gas sensing application", *Chem. Phys. Lett.*, **763**, 138204. https://doi.org/10.1016/j.cplett.2020.138204.

Vahidi Pashaki, P., Pouya, M. and Maleki, V.A. (2018), "High-speed cryogenic machining of the carbon nanotube reinforced nanocomposites: Finite element analysis and simulation", *Proceedings of the Institution of Mechanical Engineers, Part C: J. Mech. Eng. Sci.*, **232**(11), 1927-1936. https://doi.org/10.1177/0954406217714012.

Wang, Y., Li, F.-M. and Wang, Y.-Z. (2015), "Nonlinear vibration of double layered viscoelastic nanoplates based on nonlocal theory", *Physica E*, **67**, 65-76. https://doi.org/10.1016/j.physe.2014.11.007.

Wong, K., Chuan, M., Chong, W., Alias, N., Hamzah, A., Lim, C. and Tan, M. (2019), "Modeling of low-dimensional pristine and vacancy incorporated graphene nanoribbons using tight binding model and their electronic structures", *Adv. Nano Res., Int. J.*, **7**(3), 20-39. http://doi.org/10.12989/anr.2019.7.3.209.

Zenkour, A.M. (2016), "Buckling of a single-layered graphene sheet embedded in visco-Pasternak", *Adv. Nano Res., Int. J.*, **4**(4), 309-326. http://doi.org/10.12989/anr.2016.4.4.309.